Received: 12 January 2019 | Revised: 21 August 2019 | Accepted: 22 October 2019

DOI: 10.1002/qj.3688

Quarterly Journal of the Royal Meteorological Society RMetS

INCOMPASS SPECIAL COLLECTION

Spatial and temporal variability in energy and water vapour fluxes observed at seven sites on the Indian subcontinent during 2017

G. S. Bhat[1,2] | R. Morrison[3] | C. M. Taylor[3,4] | B. K. Bhattacharya[5] | S. Paleri[1] | D. Desai[5,6] | J. G. Evans[3] | S. Pattnaik[7] | M. Sekhar[8] | R. Nigam[5] | A. Sattar[9] | S. S. Angadi[10] | D. Kacha[11] | A. Patidar[12] | S. N. Tripathi[13] | K. V. M. Krishnan[13] | A. Sisodiya[7]

[1]Centre for Atmospheric and Oceanic Sciences, Indian Institute of Science, Bengaluru, India

[2]Divecha Centre for Climate Change, Indian Institute of Science, Bengaluru, India

[3]Centre for Ecology and Hydrology, Wallingford, UK

[4]National Centre for Earth Observation, Wallingford, UK

[5]Agriculture and Land Eco-system Division (AED), Space Applications Centre, ISRO, Ahmedabad, India

[6]Department of Physics, Electronics and Space Sciences, Gujarat University, Ahmedabad, India

[7]School of Earth, Ocean and Climate Sciences, IIT Bhubaneswar, Bhubaneswar, India

[8]Department of Civil Engineering, Indian Institute of Science, Bengaluru, India

[9]Dr. Rajendra Prasad Central Agricultural University, Samastipur, India

[10]Department of Agronomy, University of Agricultural Sciences, Dharwad, India

[11]Main Rice Research Station Nawagam, Anand Agricultural University, Anand India

[12]Regional Research Station-CAZRI, Jaisalmer, India

[13]Department of Civil Engineering, IIT Kanpur, Kanpur, India

Correspondence
G. S. Bhat, Centre for Atmospheric & Oceanic Sciences, Indian Institute of Science, Bengaluru-560012, India.
Email: bhat@iisc.ac.in

Funding information
Ministry of Earth Sciences; Natural Environment Research Council, NE/L013819/1

Abstract

Under the INCOMPASS project, state of the art eddy-covariance based surface flux measurement systems were installed at eight locations across India. These sites cover different climatic conditions, land use and land cover, and water management practices. Here we present the initial analysis of the measurements taken at seven sites mainly focusing on the year 2017, quantifying for the first time the remarkable contrasts in evaporative fraction across the seasons, climate zones and land management practices of the Indian subcontinent. With the exception of Jaisalmer which is the driest of the places studied, all the sites maintain values of evaporative fraction above 0.5 after the monsoon through to November. By contrast, for those sites with natural vegetation or rain-fed agriculture, evaporative fraction remains below 0.3 for the dry January–May period. In the middle Gangetic Plain area, irrigation and pre-monsoon showers together maintain evaporative fraction above 0.5 between January and June. It is also observed that different variables exhibit different intraseasonal variation characteristics even at one site. Except for Samastipur which is situated in the middle Indo-Gangetic Plains, wind speed shows spectral peak at a smaller time-scale compared to sensible and latent heat fluxes.

KEYWORDS

eddy-covariance flux, Indian monsoon, land-surface processes, evaporative fraction, surface energy balance, surface fluxes

1 | INTRODUCTION

Land surface temperature (LST) increases across India between March and May (the dry season, Figure 1) which is followed by 76% of the annual rainfall in the next 4 months (wet or summer monsoon season). A consequence of this is large changes in vegetation cover from pre-monsoon to monsoon to post-monsoon months (Figure 1). Changes in land surface characteristics influence precipitation via energy partitioning at the land–atmosphere interface, moisture supply, boundary-layer properties and local atmospheric circulation (e.g. Yasunari, 2006; Taylor *et al.*, 2011; Niyogi, 2019). This happens on multiple time and space scales; feedbacks are intimately linked to space–time variability in antecedent rainfall via changes in fast (surface soil moisture) and slower (root zone moisture and leaf area) dynamics, which in turn influence the land–atmosphere fluxes. Modelling studies have shown that simulation of active and weak spells of rainfall over central India are more realistic when surface soil moisture is determined interactively than prescribing a fixed hydrology (Rajendran *et al.*, 2002). Variations in soil moisture over certain parts of the Indian sub-continent have a strong influence on precipitation (e.g. Koster *et al.*, 2004). The dynamics of interaction between soil moisture and circulation over the northwestern semi-arid areas produces a slow northwestward migration of the monsoon even if sea-surface temperature and solar insolation are held at May climatological values (Bollasina and Ming, 2013). Including the irrigation effects in models gives more realistic spatial distribution of LST and surface pressure over the northern plains (e.g. Saeed *et al.*, 2009).

Three monsoon field programmes were conducted over the subcontinent to understand land-surface processes during the monsoon vis-à-vis their representation in models. The Monsoon Trough Boundary Layer Experiment (MONTBLEX) was aimed at understanding the structure of the atmospheric boundary layer (ABL) across the extent of the monsoon trough, the study of eddy fluxes and energetics, and the formulation of better parametrization schemes for the boundary layer for use in atmospheric general circulation models (e.g. Sikka and Narasimha, 1995; Bhat and Narasimha, 2007). The Land Surface Processes Experiment (LASPEX-97) carried out over the Sabarmati river basin in northwest India in 1997 aimed to quantify land–atmosphere exchanges during different seasons (Sastry *et al.*, 2001). The Continental Tropical Convergence Zone (CTCZ) programme, carried out over the main monsoon zone during 2009–2012, had a component on hydrology and land surface processes involving observations and modelling (CTCZ, 2008). These observational studies have provided some detailed measurements of the monsoonal boundary layer (e.g. Bhat and Narasimha, 2007) and insights into seasonal changes in the partitioning of surface fluxes (e.g. Sastry *et al.*, 2001).

One major omission in the past monsoon campaigns concerns the quantification of latent-heat flux (LH). LH was either estimated from the gradient method (e.g. Padmanabhamurty and Saxena, 2001) or indirectly (Sinha and Pillai, 2001). Accurately measured data on the co-evolution of sensible-heat flux (SH) and LH at the season transitions from pre-monsoon to monsoon to post-monsoon periods are not yet available. Irrigation potential in the northern plains of the Indian subcontinent is among the highest in the world (e.g. Saeed *et al.*, 2009; www.fao.org) and is extensively practised (Rodell *et al.*, 2009), but its effects on surface energy partitioning are not quantified. Therefore, in the INCOMPASS programme (Interaction of Convective Organisation with Monsoon Precipitation, Atmosphere, Surface and Sea: Turner *et al.*, 2019), accurate measurement of LH and SH by deploying state-of-the-art sensors and instruments was given high priority. Eddy covariance (EC) flux systems were installed at eight locations across India (Table 1) between October 2015 and June 2016. This study reports the monthly and seasonal variation in SH and LH at seven sites (Figure 2), mainly focusing on the year 2017 since data during different seasons of the year are available. Section 2 gives site selection, instrument details, data quality control and method of flux calculations, followed by flux time series in Section 3. Section 4 contains discussions and Section 5 conclusions.

2 | FIELD SET-UP AND FLUX ESTIMATION

2.1 | Site selection

Surface types show strong geographical variability over the Indian subcontinent from the dry Thar Desert of northwest India to the humid and forested regions of the northeast, between which lie the fertile alluvial soils of the northern plains where irrigation is widespread. There is large north–south and east–west contrast in precipitation (Figure 2) and vegetation characteristics (Figure 1). Large variations in natural vegetation and crop practices called for sampling in different land surface and/or climatic conditions. EC systems have been installed at eight sites under the INCOMPASS programme that cover a range of surface and climate conditions (Figure 2, Table 1, Appendix S1), heralding a step change in land surface

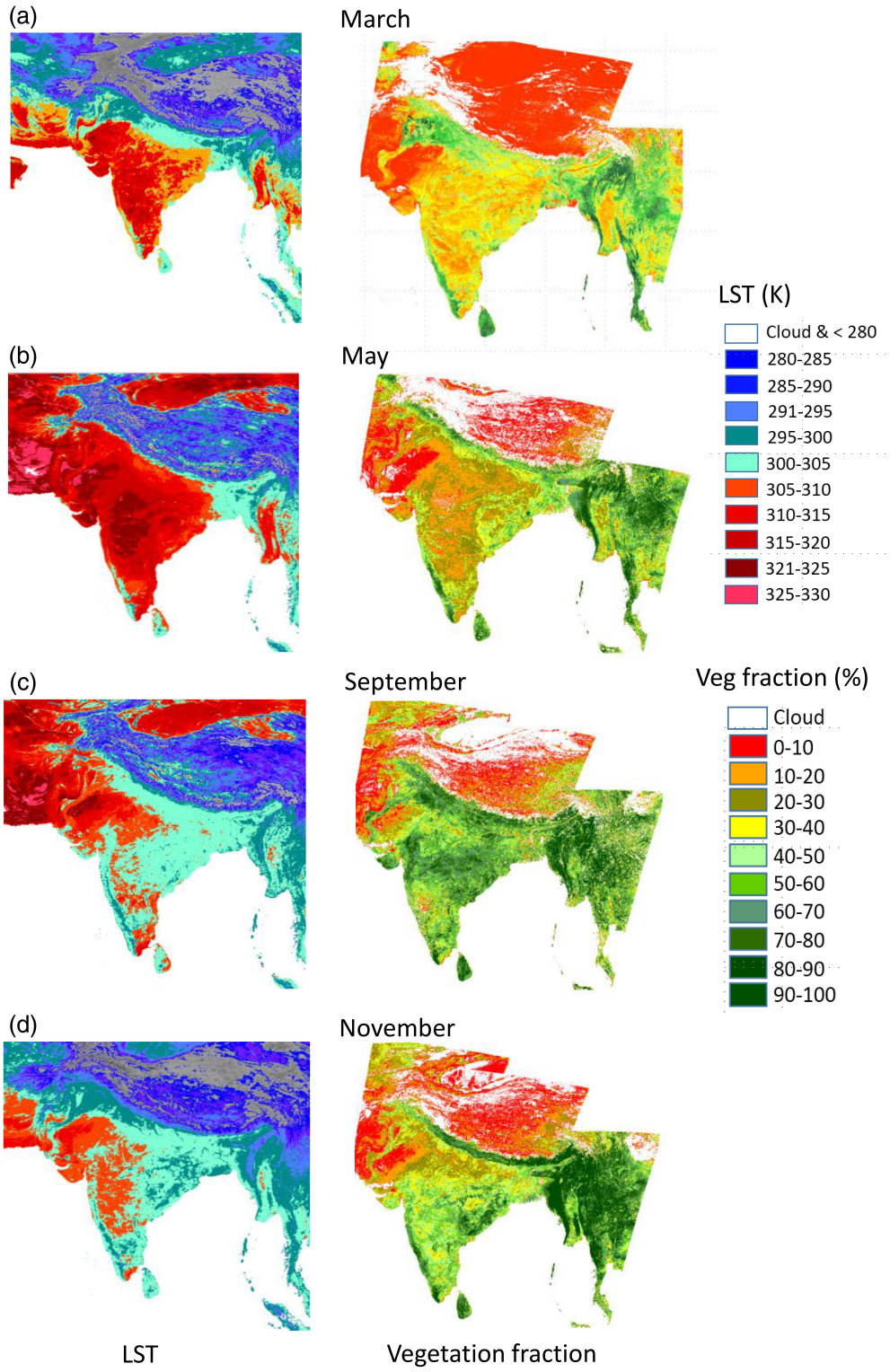

FIGURE 1 Left panels: Land surface temperature (LST) from MODIS; right panels: vegetation cover derived from OCM-2 satellite data. (a) March; (b) May; (c) September; (d) November. Colour bars on right are common to respective variables. LST is MODIS LST collection 6 (product code MOD11C3: Wan, 2014). Vegetation fraction is taken from http://www.bhuvan.nrsc.gov.in

observations in India (see e.g. Baldocchi *et al.*, 2001; Sundareshwar *et al.*, 2007).

The easternmost site is located in the Indian Institute of Technology (IIT) Bhubaneswar campus which lies in the path of monsoon low-pressure systems. The site has natural vegetation to its west and south, and rain-fed agricultural land to the east and north. The site at Samastipur is in a vast agricultural field belonging to Dr. Rajendra Prasad Central Agricultural University, situated in the middle Indo-Gangetic Plains. Irrigated rice and wheat are dominant crops grown during summer and winter seasons, respectively. The site at Kanpur is in the IIT Kanpur campus and surrounded by natural grass that can grow taller than 2 m. During the monsoon season, standing

TABLE 1 Details of INCOMPASS EC-flux sites depicted in Figure 2

Place	Lat. (°N)	Lon. (°E)	Alt. (m)	June–Sep. average rainfall (mm)	Land characteristics
Bengaluru	13.02	77.57	910	415	Natural vegetation
Berrambadi	11.76	76.59	870	220	Mixed agriculture
Bhubaneswar	20.15	85.68	60	975	Natural vegetation in upstream wind direction during monsoon, rain-fed agriculture downstream
Dharwad	15.50	74.99	693	485	Agriculture farm
Jaisalmer	26.99	71.34	196	120	Natural sewan grass
Kanpur	26.51	80.22	128	600	Natural grassland
Nawagam	22.80	72.57	55	550	Agriculture (rice)
Samastipur	26.00	85.67	39	850	Agriculture (rice and wheat)

EC systems were established at eight sites for INCOMPASS. This article reports observations made at all sites except Berrambadi.

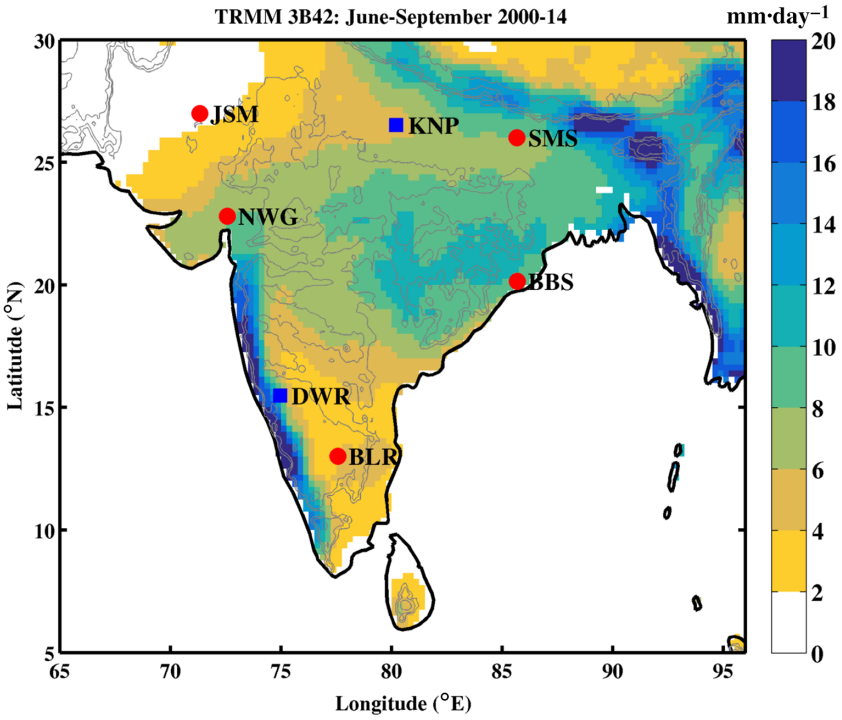

FIGURE 2 INCOMPASS flux sites. Colour shade is average June–September daily average rainfall based on TRMM 3B42 product for the period 2000 to 2014. Precipitation over ocean has been masked. Contour lines are orography at 300 m interval. BBS, Bhubaneswar; BLR, Bengaluru; DWR, Dharwad; JSM, Jaisalmer; KNP, Kanpur; NWG, Nawagam; SMS, Samastipur. Irgason EC system and LI-COR EC system are shown by filled red circles and filled blue squares, respectively

water is often present below the grass canopy. There is an irrigation canal nearby, and the site becomes flooded when excess water is let out of the canal. The site at Jaisalmer is in the campus of the Central Arid Zone Research Institute (CAZRI), on flat terrain and in the midst of natural vegetation, mostly consisting of sewan grass, the main grass variety of this region. Nawagam tower is in a rice field belonging to the Main Rice Research Station of the Anand Agricultural University. Here rice is grown during summer and the fields contain standing water from the transplantation to the grain-filling period. The winter crop could be irrigated wheat or rice, and in some years nothing is grown, as in the winter of 2017. The Dharwad site is located on the campus of the University of Agricultural Sciences and has rain-fed crops. The site in Bengaluru is surrounded by natural vegetation (shrubs and trees less than 6 m tall).

Type of soil, vegetation cover, land-use/land-cover (LULC) influence surface energy partitioning. Photographs taken at flux sites in different seasons along with information on site characteristics derived from satellite measurements are given in Appendix S1. Some of the photographs show soil texture and others give some basic idea about the fetches and vegetation cover. It is

worth noting here that population pressure is very high in India, and any flat land, where available, is used for agriculture/plantation. Land holding is often small, and trees are planted at the boundary of each plot. Except for the surface flux community, no-one else likes a vast open area without trees, and trees are planted where flat land with an open area existed and was not used for growing crops. Safety of instruments is another issue. Given these constraints, getting a site with fetches of more than 25 is a challenge in India, and INCOMPASS flux sites have some of the best exposures in India.

2.2 | Instruments and data processing

Three-dimensional sonic anemometer–thermometers and open path CO_2–H_2O gas analysers are common to all EC sites. EC150 (Irgason) systems (Campbell Scientific Inc., Logan, UT, USA) are installed at five sites (Bhubaneswar, Bengaluru, Jaisalmer, Nawagam and Samastipur). LI7500A gas analyser (LI-COR Biosciences Inc., Lincoln, NE, USA) and Gill Windmaster sonic anemometer systems are deployed at three other sites (Table 1). Measurement heights are ∼8 and ∼5 m above ground at the EC150 and LI7500A flux sites, respectively. Existing 10 m masts set up for Agro-Met Stations (AMS) under an ISRO-GBP programme (Bhattacharya *et al.*, 2009; 2013; Singh *et al.*, 2014; Shweta *et al.*, 2018) are utilized at Jaisalmer, Nawagam and Samastipur, and the rest are set up exclusively under the INCOMPASS programme. Eddy covariance sensors were newly procured (the majority of them in 2016) and factory calibrated. No further calibrations of sensors were performed in 2017 except for periodically cleaning the sensor heads and changing the gas analyser chemicals after a year. Absence of a temporal trend in water vapour concentration suggested that there is no noticeable sensor drift in gas analysers during the data collection period.

Raw data are archived at 20 Hz and all processing is done post-facto. A common EddyPro® Flux Software (Fratini and Mauder, 2014; LI-COR Biosciences, 2017) based processing method with an averaging time interval of 15 min has been adopted for all EC flux calculations. Fluxes that passed all the statistical tests, were above specified quality thresholds and were considered to be good for surface energy balance calculations are retained in subsequent analysis. To ascertain the seasonal evolution of SH and LH, 5-day running averages are constructed (henceforth, pentad averages). Further details on the EC flux calculations are given in Appendix S2.

Kipp & Zonen CNR4 and Hukseflux NR01 net radiometers have been installed at the Campbell and LI-COR EC sensor-based flux sites, respectively. From measured incoming short-wave (SW_{in}), reflected short-wave (SW_{out}), incoming long-wave (R_{in}) and outgoing long-wave (R_{out}) components of radiation, net radiation (R_{net}) is obtained from

$$R_{net} = SW_{in} + R_{in} - (SW_{out} + R_{out}). \quad (1)$$

Reliable radiation data are available at Jaisalmer, Nawagam and Samastipur from July 2017 after the installation of new radiation instruments, and from the beginning of 2017 at other sites. Because SH and LH are caused by turbulence in the ABL, their sum is called turbulent heat flux (THF). R_{net} drives other surface fluxes, and the surface energy balance over land takes the form (Garratt, 1992):

$$R_{net} = THF + GHF + Q_{cs} + Q_{adv}, \quad (2)$$

where GHF is ground heat flux, Q_{cs} is canopy storage (heat and chemical energy) and Q_{adv} is horizontal advection of heat. R_{net} toward the surface, and SH, LH and GHF away from the surface, are taken as positive. GHF is positive during the daytime and negative during the night-time; daily average GHF is small compared to the corresponding THF (e.g. the former and the latter are less than 5 and ∼150 $W \cdot m^{-2}$ on a clear-sky day during summer at Kanpur). Note that over an irrigated land surface with standing water, e.g. an irrigated rice field, water may not be stagnant but slowly moving and may advect sensible heat which is normally not included in Equation 2. We will also study evaporative fraction (EF) and residual flux (RESF) to characterize land surface processes. These are defined by

$$EF = LH/THF, \quad (3)$$

$$RESF = R_{net} - (THF + GHF). \quad (4)$$

2.3 | Horizontal variations and seasonal changes

In making surface flux measurements, fetch and exposure are important considerations (Horst and Weil, 1994; Lemone *et al.*, 2007; Fall *et al.*, 2011). The EddyPro software derived footprints (Kljun *et al.*, 2004; Li-COR Biosciences, 2016) at different sites are given in Table 2. The footprints shown correspond to the upwind distance within which 90% of the turbulent fluxes measured with the EC flux sensors originate. The EddyPro® software derived footprint depends on the sensor height, surface layer stability, and surface roughness (Kljun *et al.*, 2004). Footprints are shorter and longer under unstable and stable conditions, respectively. Normally the surface layer over land in the Tropics is unstable during daytime and stable during the

TABLE 2 Average daytime (0900–1700 IST) and night-time (1900–0600 IST) flux footprints and their respective standard deviations in the year 2017

Flux site	Daytime footprint(m)	Daytime footprint std(m)	Night-time footprint(m)	Night-time footprint std (m)
Bengaluru	230	60	360	440
Bhubaneswar	320	370	1,275	1,410
Dharwad	280	170	1,000	890
Jaisalmer	250	90	1,010	1,350
Kanpur	310	345	1,250	1,100
Nawagam	230	165	930	1,150
Samastipur	340	410	1,250	1,400

Flux footprints of more than 5,000 m have been removed while averaging. Here, flux footprint represents the cumulative upwind distance from the tower that contributed 90% of the observed flux for each 15 min flux averaging interval.

night. The major fraction of THF over land is generated during the daytime. In view of this, day and night-time footprints are shown separately. The average daytime footprint varies between 230 and 340 m (i.e. 30 to 40 times the measurement height) while night-time values are around 1 km except at Bengaluru. In order to provide a better idea about the horizontal variations in surface conditions around flux sites, Landsat-derived LST on a clear-sky day during March, October and November, photographs taken during different times of the year and a Google map indicating the flux tower position are given in Appendix S1. LSTs shown have been retrieved from Landsat 8 data (https://earthexplorer.usgs.gov) on clear-sky days in the months of March, October and November of 2016 and 2017 using split thermal infrared channels centred at 10.5 μm (band 10) and 11.5 μm (band 11) wavelengths. A split-window technique that involves corrections for water vapour absorption from differential response in split window channels (Ren *et al.*, 2015) and surface emissivity correction based on vegetation index derived from red (band 4) and near-infrared (band 5) bands of Landsat 8 is used (Rajeshwari and Mani, 2014).

3 | RESULTS

The major focus in this study is on getting quantitative numbers for the LH and SH fluxes in different seasons, and similarities and contrasts across the sites. Therefore, pentad time series and monthly variations at all sites will be discussed together. Figures 3–9 show observed temporal variations of THF, R_{net}, SH, LH, τ and CO_2 fluxes along with rain-gauge measured and satellite-data derived daily rainfall at Bhubaneswar, Bengaluru, Dharwad, Jaisalmer, Kanpur, Nawagam and Samastipur, respectively. Monthly average daytime (0900 to 1600 h local time) fluxes and their standard deviations are shown in Figures 10 and 11, respectively. Rain-gauge measured June to September (January to May) rainfalls at these sites in the year 2017 are 1236 (74), 573 (290), 343 (120), 139 (20), 493 (38), 842 (22) and 938 (193) mm, respectively. Figures 3–11 bring out spatial differences, seasonal changes and the role of irrigation on surface turbulent fluxes. THF follows R_{net} (panels a) in Figures 3–9 at all locations, with the former being higher except on a few occasions. Thus, seasonal evolution of THF and its sub-seasonal variations are closely tied to those of R_{net} (e.g. Figures 3a and 7a), whereas partitioning of R_{net} between LH and SH (panels b) in Figures 3–9 is sensitive to LULC. At sites with natural vegetation (e.g. Bengaluru and Jaisalmer) and rain-fed agriculture (e.g. Dharwad), SH dominates the THF during January to May, which is also reflected in the low values of EF (panels c) in Figures 3–9 and 10d. This pattern is interrupted by rainfall, following which EF increases rapidly and then returns to pre-rainfall values over a period that depends on the amount of daily rainfall and land surface characteristics. For example, at the semi-arid Jaisalmer, the entire pre-monsoon season precipitation is 20 mm with the maximum daily rainfall of 9 mm and EF decreases to values below 0.2 within 10 days of rainfall (Figure 6c), while at Bhubaneswar (Figure 3c) and Bengaluru (Figure 4c) where the maximum daily rainfall is ~40 mm, the rain effect lasted for about a month. Kanpur has natural grass but outflow from a nearby canal increases soil moisture. This is evident during March–April (Days 70 to 120; for convenience of reference, Day of the Year is called Day) where LH dominates THF (Figure 7a,b) and EF increased from ~0.5 to 0.8 (Figures 7c and 10d) in the absence of any detectable rainfall. Negative CO_2 flux during this period (Figure 7d) is owing to the vegetation growth as adequate soil moisture was available. SH and LH are comparable

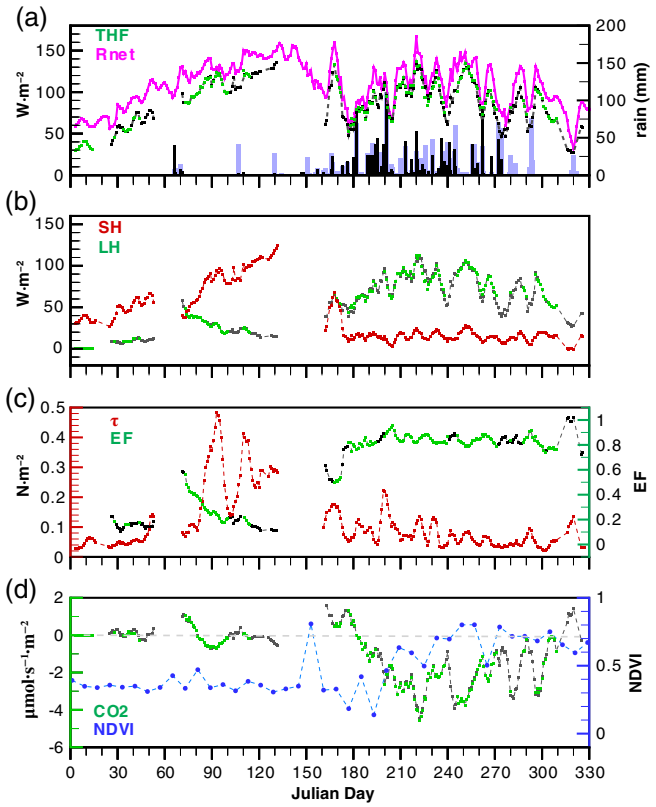

FIGURE 3 Five-day running averages at Bhubaneswar. (a) Turbulent heat flux (THF) and net radiation (R_{net}). (b) SH and LH. (c) Shear stress (τ) and EF. (d) CO_2 flux and Normalized Difference Vegetation Index (NDVI). For THF, LH, SH, EF and CO_2 flux, green colour symbols mean data passed through all quality criteria and sample size in pentad averaging is more than 67% of the maximum number possible. When data are interpolated and/or pentad averaging sample size has less than 67% of maximum possible, then it is shown by black colour symbols. In panels (c) and (d), colours of the vertical axes correspond to those of respective variables. Bars in panel (a) show daily precipitation (refers to the axis on right); black and light blue colour bars are rain-gauge measured and satellite-data derived precipitation, respectively

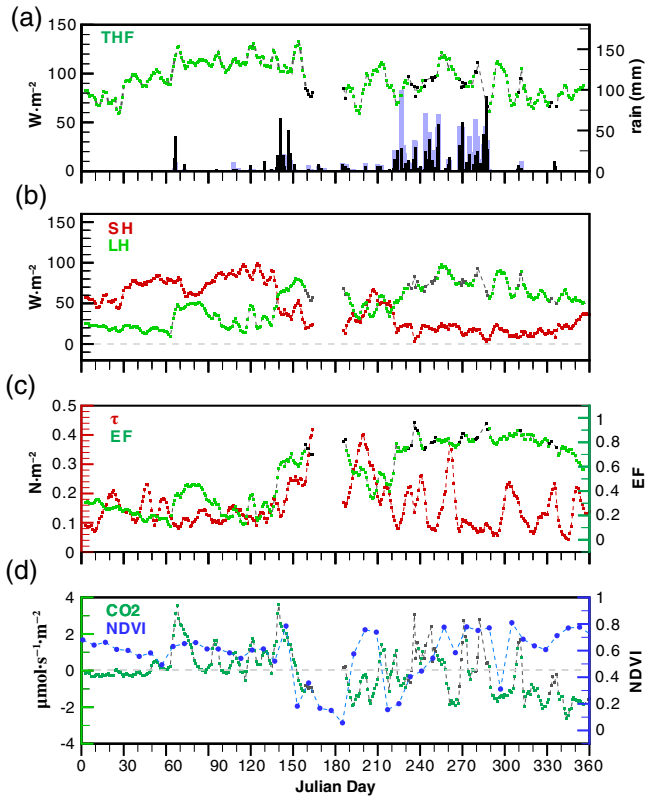

FIGURE 4 Same as Figure 3 but for Bengaluru except that R_{net} is missing

at Nawagam until Day 120 (January to April,) and then LH started increasing while SH decreased and the change was not related to rainfall (Figure 8b). The entire field at Nawagam was irrigated for about 15–20 days in the month of May for growing short-duration green manure, leguminous to maintain soil fertility. At Samastipur, LH dominates SH throughout the year and EF exceeded 0.8 between Days 40 and 90 (Figures 9b,c and 10d) which is due to irrigated wheat cultivation which is also reflected in the large negative values of CO_2 flux during the corresponding period (Figures 9d and 10e). EF remained above 0.5 after harvesting also and it rose to 0.8 once pre-monsoon showers started (on Day 110). Thus, the combined effect of irrigation and pre-monsoon rainfall maintained high EF at Samastipur during January to May (Figure 10).

Once monsoon rains commenced (between Days 150 and 180 depending on the site's geographic location), SH decreased below 20 $W \cdot m^{-2}$ at Bhubaneswar, Kanpur, Nawagam and Samastipur, and EF often remained above 0.7 (Figure 10d). These high values continue until November, and at some sites, beyond. Bengaluru is in the rain-shadow region of the Western Ghats and here rainfall during Days 150 to 210 (i.e. in June and July) is less compared to even May, and SH becomes comparable to LH or exceeds it. From August onwards, Bengaluru started getting frequent rainfall in 2017, SH reduced and EF fluctuated around 0.8 during the next 4 months (Figure 4c). At Jaisalmer, SH dominates THF, LH increases for brief periods following rainfall but the effect does not last for more than a couple of weeks (Figure 6b). SH and LH are out of phase and as a consequence, intraseasonal variations in SH, LH and EF are strong here. During July to September (Days 181–273), EF is more than 0.85 at Samastipur (Figures 9c and 10d). The standard deviation of daytime SH somewhat mimics the variation of mean SH, especially during the monsoon season (Figure 11a). Such a clear separation is not seen in the standard deviation of daytime LH (Figure 11b).

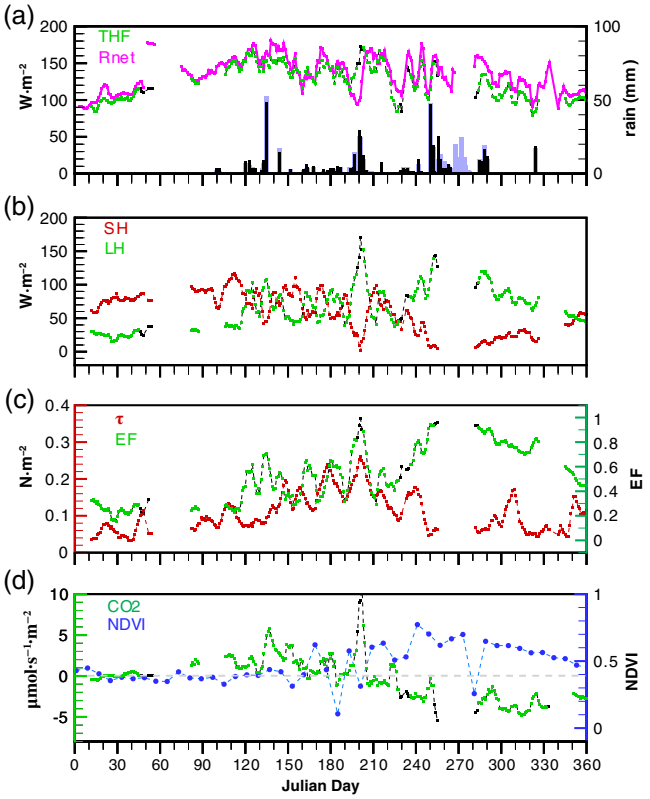

FIGURE 5 Same as Figure 3 but for Dharwad

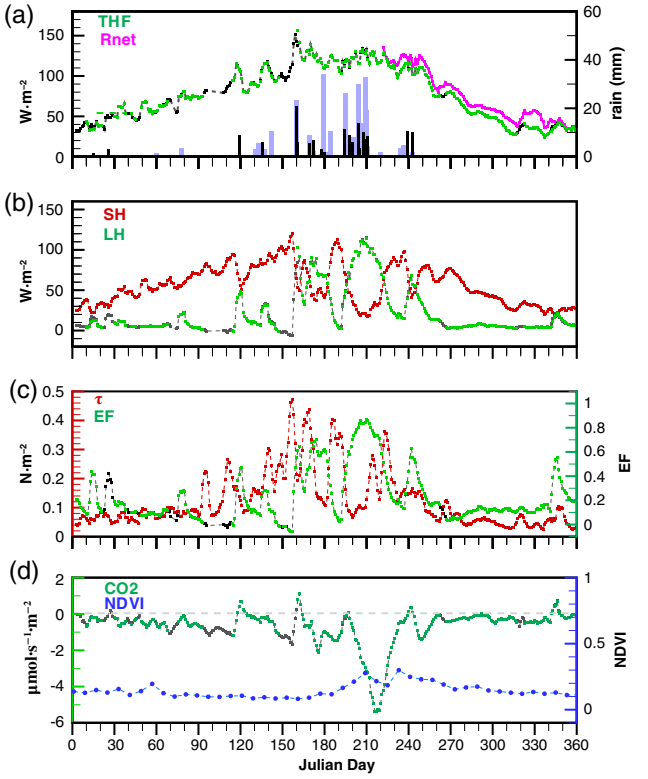

FIGURE 6 Same as Figure 3 but for Jaisalmer

It is also seen that EF exceeded unity on a few occasions at Kanpur, Nawagam and Samastipur, which we verified is not owing to measurement error. On these occasions, pentad average SH becomes negative, evaporation rates are high, wind speed happens to be above average but with or without any major shift in wind direction. This could be a result of horizontal advection of warm (and dry) air, or instability of a stratified shear layer above the ABL (Bhat and Fernando, 2016). A detailed analysis is required to understand the actual mechanism, which we hope to carry out.

Shear stress (τ) shows a kind of east–west divide in the northern plains of India with Kanpur (Figure 7c), Samastipur (Figure 9c) and Bhubaneswar (Figure 3c) having lower values compared to Jaisalmer (Figure 6c) and Nawagam (Figure 8c) during the monsoon season. The intraseasonal time-scales of τ seem to be smaller than those of SH and LH (e.g. Jaisalmer, Figure 6). To confirm this, we show in Figure 12 spectra of measured fluxes at four stations (Jaisalmer, Kanpur, Nawagam and Samastipur) having best continuity in pentad time series among the seven sites. Across the sites, the primary mode in τ is at less than 30 day time-scale (Samastipur is an exception), whereas primary modes of SH/LH are above 30 days. At Jaisalmer and Samastipur, peaks in SH and LH coincide, whereas the two are well separated at Kanpur (Figure 12b) and Nawagam (Figure 12c). CO_2 flux peaks at 84 days at Nawagam and Samastipur, while it is at 43 days at Jaisalmer and between 40 and 60 days at Kanpur, suggesting a shorter period for natural grass compared to that for rice (and wheat). If these are climatological features of respective sites or only for the year 2017 needs to be understood by studying data of other years.

Solar insolation at the top of the atmosphere is the same at Samastipur, Kanpur and Jaisalmer since they are nearly at the same latitude. Given that THF follows R_{net} closely, differences in the former point to differences in the latter. Daytime THF in April 2017 are 272, 477 and 385 $W \cdot m^{-2}$ at Jaisalmer, Kanpur and Samastipur, respectively (the corresponding THF in May are 269, 447 and 349 $W \cdot m^{-2}$). THF at Jaisalmer is ~57% of that at Kanpur, clearly indicating that far less R_{net} is available at Jaisalmer compared to that at Kanpur. *In situ* radiation measurements give an albedo of 24% at Jaisalmer compared to ~15 and 10%, respectively, at Kanpur and Samastipur in the year 2017. Net long-wave cooling is larger at Jaisalmer compared to the other two sites due to less columnar atmospheric water vapour. Thus, small R_{net} at Jaisalmer is the combined effect of higher surface albedo and net long-wave cooling.

In understanding land surface processes, soil temperature, soil moisture (SM) and GHF are important. Among

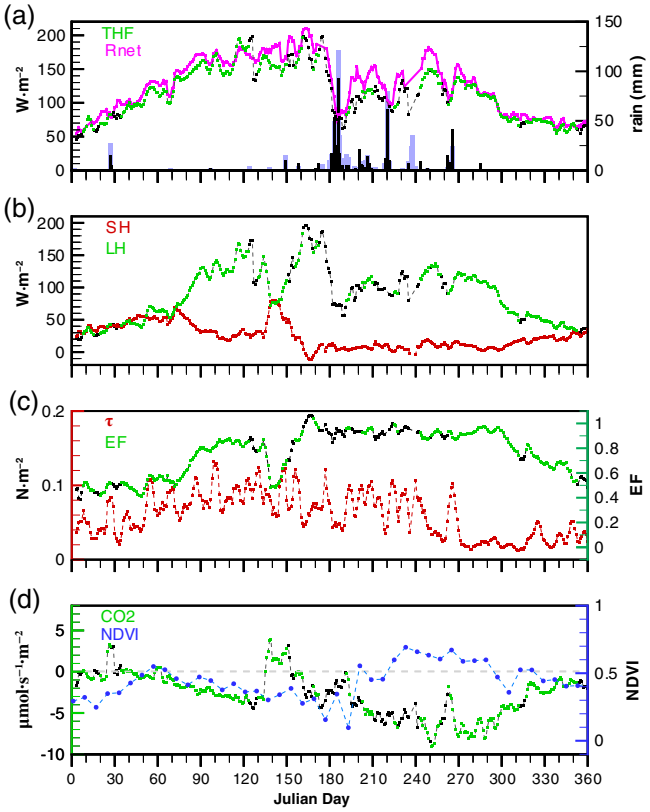

FIGURE 7 Same as Figure 3 but for Kanpur

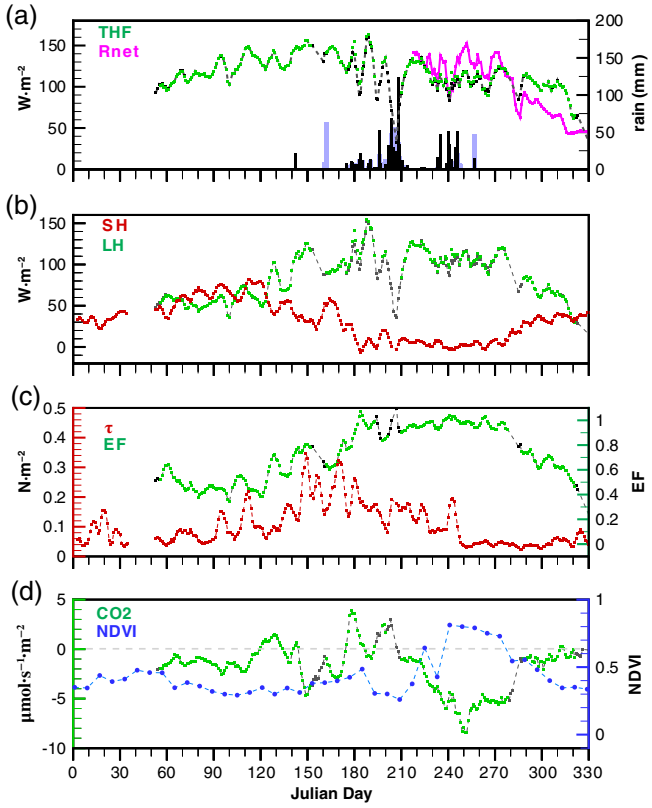

FIGURE 8 Same as Figure 3 but for Nawagam

the seven INCOMPASS flux sites, these variables were measured at Dharwad and Kanpur. Figure 13 shows the 5-day running average of GHF, soil temperature and SM, all measured at 5 cm depth (GHF into the soil is positive). Between January and the last week of April, positive and gradually increasing GHF reaching up to 18 $W \cdot m^{-2}$ is seen at Dharwad; thereafter it fluctuates on intraseasonal time-scales about a mean value of zero and the maximum amplitude is less than 10 $W \cdot m^{-2}$ (Figure 13a). At Kanpur, positive GHF starts in March and continues until mid-June, i.e. until the monsoon arrives. Soil continuously loses heat at Kanpur from September onwards. Compared to THF (Figure 5a), GHF (Figure 13a) is less than 10% at Dharwad; however, it became ~15% in March and April. GHF is ~10% or less compared to THF at Kanpur (Figure 7a, Figure 13a). Therefore, neglecting GHF can introduce an error of up to 15% in the surface energy balance in the 5-day running average. Soil temperatures at Dharwad and Kanpur peak in April and June, respectively, which are consistent with respective GHF variations (Figure 13b). SM at Dharwad was low and varied between 6 and 8% during January to April (confirming the absence of irrigation) and then increased following pre-monsoon showers in May (Figure 13c). High soil moisture at Kanpur in January and February is due to seepage of water from a nearby irrigation canal and its effect lasted until April.

Figure 14 shows RESF at Dharwad and Kanpur. RESF and GHF are of comparable magnitude the majority of the time; however, the amplitude of variations in RESF can be much larger, especially around the times when it rains, due to two reasons. Gas analyser signal strength deteriorates during rains or when raindrops cover the sensor head, and we have removed these samples. This leads to a larger number of missing data points in the process and accuracy of the pentad THF is less during such periods. Downdraughts and cold outflow from moist convection (Knupp and Cotton, 1985) can produce large temperature gradients locally, and horizontal advection may become important around rain events. The extreme values seen in the scatter plot of R_{net} vs. THF+GHF (Figure 14c,d) are mostly associated with convection.

4 | DISCUSSION

Despite past modelling and field efforts, current numerical weather models are unable to simulate the spatial and temporal distribution of monsoon rainfall over the Indian subcontinent (Rajeevan *et al.*, 2012). Direct comparison between field experiment time-series data and

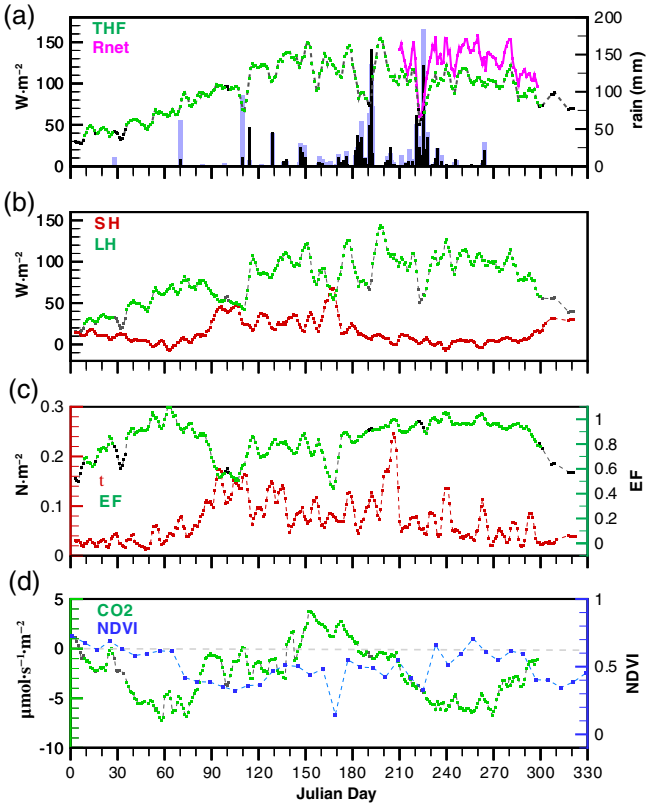

FIGURE 9 Same as Figure 3 but for Samastipur

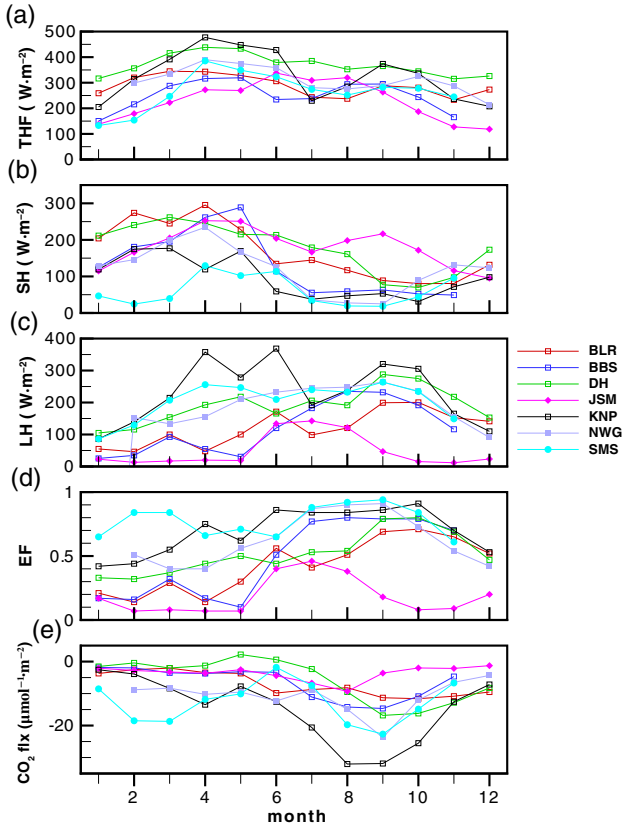

FIGURE 10 Daytime (0900–1600 LT) monthly averages. (a) Sensible-heat flux, (b) latent-heat flux, (c) turbulent-heat flux, (d) evaporative fraction, (e) CO_2 flux

model data from nearby grid points in data assimilation and forecast systems has proved very useful in identifying systematic errors in the model physical parametrizations and in developing improved parametrizations (Betts *et al.*, 1998). INCOMPASS observations have provided an unprecedented time series of surface SH, LH, τ and CO_2 over the Indian landmass, covering different climates and LULCs. They quantify, for the first time in India, the remarkable contrasts in EF across the seasons, climate zones and land management practices of the subcontinent. Three of the sites benefit from irrigation, and this raises EF at the monthly time-scale to above 0.8, and even above 1 over short periods. These high values contrast with the two natural landscapes sampled, where monthly mean EF does not exceed 0.7. Given the extent of irrigation practices across India, coupled with the influence of surface fluxes on the atmosphere, this suggests an important impact of large-scale irrigation on the atmosphere outside of the core monsoon, consistent with various modelling studies (e.g. Saeed *et al.*, 2009). With the exception of the driest site (Jaisalmer), all the sites maintain values of EF above 0.5 after the monsoon through to November. For those sites with natural vegetation or rain-fed agriculture, EF remains below 0.3 for the January–May period.

Different rainfall conditions and water management strongly impact sub-monthly flux variations. This is clearly demonstrated in Figure 11 during the monsoon months of July to September. Sites where the vegetation has access to plentiful soil water (Samastipur, Bhubaneswar, Kanpur, Nawagam) exhibit fluctuations in SH less than half the magnitude of the other, more water-stressed sites (Jaisalmer, Dharwad, Bengaluru). Similarly, low temporal variations in SH are also observed outside the monsoon when irrigation is in operation (Samastipur in January–March, Kanpur in April). These fluctuations in SH are likely to have important feedbacks on the atmosphere. In the drier regions of India, break periods within the monsoon will be associated with sharply increased sensible-heat fluxes (and hence temperatures), while wetter areas will heat the atmosphere only weakly. The space–time variations in heating will influence low-level circulations, and potentially modulate the characteristics of intraseasonal variability (e.g. Webster *et al.*, 2002).

Because partitioning of surface energy fluxes among different components depends on LULC and water management practices, a wide variation can exist even within a single grid of a numerical weather model (e.g. 20 km × 20 km), say for example when irrigated agricultural fields, natural vegetation and other

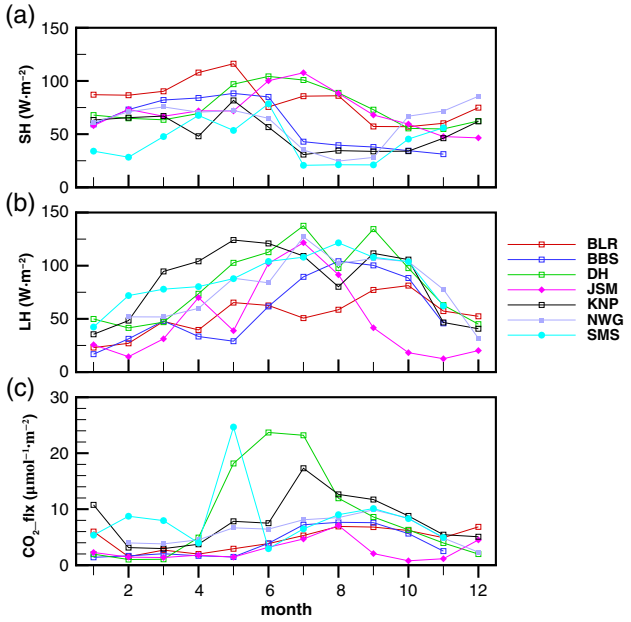

FIGURE 11 Standard deviation of monthly daytime fluxes. (a) Sensible-heat flux, (b) latent-heat flux, (c) turbulent-heat flux, (d) evaporative fraction, (e) CO_2 flux

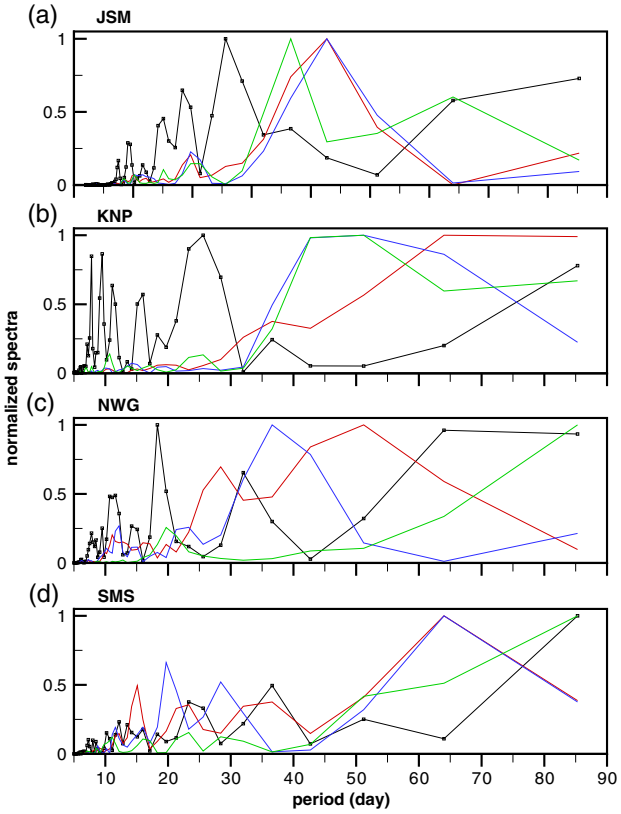

FIGURE 12 Spectra of pentad time series considering a time interval of 256 days between Days 30 and 310. (a) Jaisalmer, (b) Kanpur, (c) Nawagam, and (d) Samastipur. Black – shear stress; red – SH; blue – LH; green – CO_2 flux. Symbol is drawn on black line to indicate Fast Fourier Transform (FFT) spectral periods. Spectra are normalized by the respective maximum value in 10- to 90-day time period range to highlight relative spectral peaks on sub-seasonal time-scales

human-dominated settlements (e.g. urban areas) co-exist. Therefore, a question naturally arises about the spatial representativeness and utility of a few surface flux measurements carried out in a few locations as in the INCOMPASS programme. The climatology of the area surrounding a flux site is as important, if not more so, as the local spatial inhomogeneities. Consider the examples of Samastipur and Jaisalmer. In the Samastipur area, which lies in the Gangetic Plain where agricultural land use dominates the landscape, irrigated rice during summer and wheat during winter are common over vast stretches of the land. Jaisalmer, on the other hand, is a semi-arid landscape dominated by natural vegetation. Thus, these two flux sites have exposures closer to dominant LULC characteristics of respective areas. The Samastipur and Jaisalmer areas, respectively, receive about 1,000 and 150 mm precipitation during the summer monsoon season. Such large differences in precipitation do not occur over one grid length of any present-day general circulation model, and differences in precipitation are reflected in differences in the vertical thermal structure (e.g. strength of ABL top inversion and dryness of the free troposphere). Such differences in the mean state of the atmosphere, both within and above the ABL are important to the surface fluxes. Drier air that subsides from the free troposphere and enters the ABL affects boundary-layer humidity and thereby the surface flux partitioning (Bhat and Fernando, 2016). The horizontal footprints of thermal structure in the free atmosphere above the ABL are much larger than those of local spatial inhomogeneities and water management practices. Therefore, the fluxes measured at Samastipur and Jaisalmer are modulated by respective regional climatologies, and carry their signatures. For these reasons, the authors and a large section of the land surface, hydrological and meteorological modelling community (e.g. Williams *et al.*, 2009) are convinced that despite many practical limitations, flux measurements, even when limited to few places, do provide detailed information on flux magnitudes and insight into processes, and will be useful to validate model outputs.

Among the sites, maximum CO_2 assimilation occurs at Kanpur during the months of August and September. This means that this grassland ecosystem is absorbing more CO_2 from the atmosphere compared to rice crops at Nawagam and Samastipur. The Bengaluru site with shrubs and small tress and not much fast-growing vegetation (e.g. grass) has a lower net uptake of CO_2, most likely reflecting lower rates of photosynthesis and/or higher ecosystem respiration rates of the forested ecosystem.

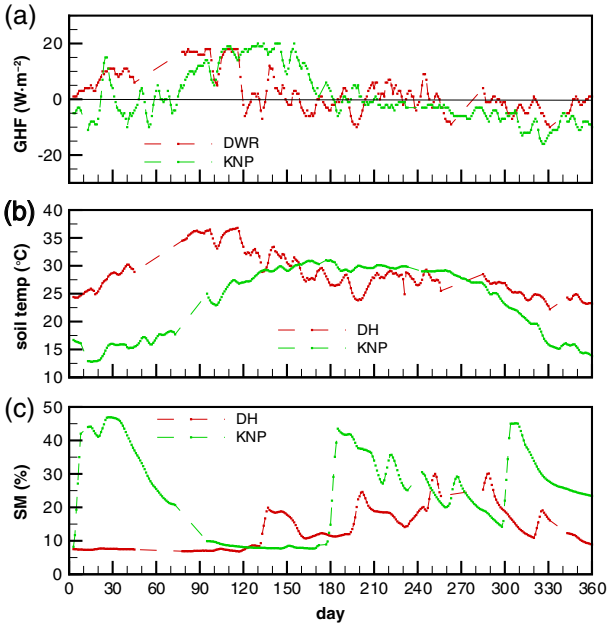

FIGURE 13 Variation of 5-day running average values at Dharwad and Kanpur in the year 2017. (a) Ground heat flux, (b) soil temperature, and (c) soil moisture. Measurement depth is 0.05 m

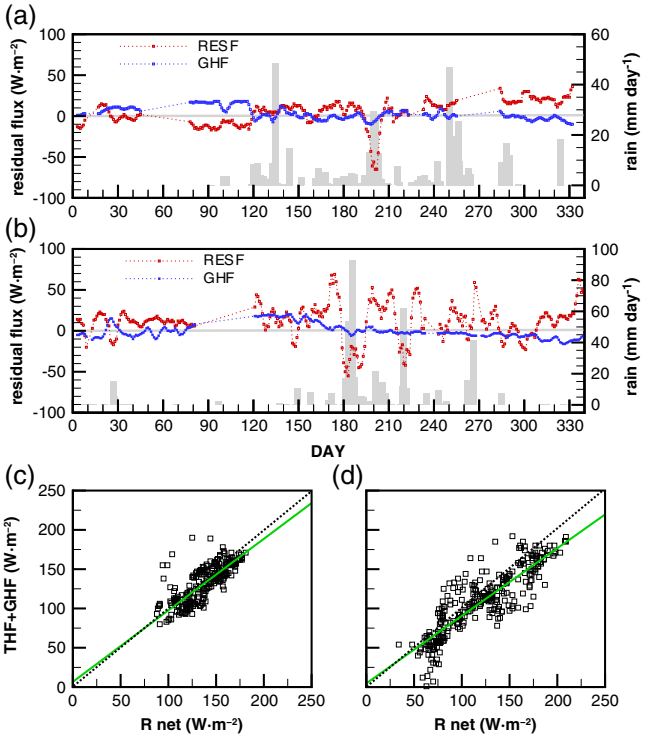

FIGURE 14 Time series of 5-day running average GHF and residual flux at (a) Dharwad, and (b) Kanpur. (c) Scatter plot of R_{net} vs. RESF at Dharwad. The dotted line has a slope of 1, and the continuous line (green) is the least square fit excluding data of days from 198 to 204; the slope of the line and the R^2 value are 0.91 and 0.72, respectively. (d) Same as (c) but for Kanpur. Slope of the best-fit line including all data points is 0.86 and the R^2 value is 0.75

5 | CONCLUSIONS

In weather prediction models, simulations of surface fluxes across India are poorly constrained by observations. The INCOMPASS programme has made a good beginning by enabling high-quality surface flux measurements over the Indian subcontinent. The study also brings out the complexity that exists across India. It is hoped that provision of high-quality land surface data from the INCOMPASS project will facilitate interrogating our models on a range of spatial and temporal scales, from the formation of convection over land to seasonal and interseasonal dynamics.

Our important findings are the following.

1. With the exception of Jaisalmer, all the sites maintain values of EF above 0.5 after the monsoon through to November. For those sites with natural vegetation or rain-fed agriculture, EF remains below 0.3 for the January–May period. In the middle Gangetic Plain area, irrigation and pre-monsoon showers together maintain EF > 0.5 between January and June.
2. The effect of rainfall on latent-heat flux can last up to a month during the pre-monsoon season except in very dry areas (e.g. Jaisalmer).
3. Different variables exhibit different intraseasonal variation characteristics. Except for Samastipur, wind speed shows a spectral peak at a smaller time-scale compared to sensible- and latent-heat fluxes.

ACKNOWLEDGEMENTS

INCOMPASS is jointly funded in the United Kingdom and India by the Natural Environment Research Council (NE/L013819/1) and the Ministry of Earth Sciences, under the Monsoon Mission, respectively. The support provided by Directors of Space Applications Centre, CAZRI and IIT Bhubaneswar, and Vice-chancellors of Dr. Rajendra Central Agricultural University and Anand Agricultural University are acknowledged.

ORCID

G. S. Bhat https://orcid.org/0000-0002-5814-5144
C. M. Taylor https://orcid.org/0000-0002-0120-3198
S. Pattnaik https://orcid.org/0000-0003-3128-6972

REFERENCES

Baldocchi, D., Falge, E., Gu, L., Olson, R., Hollinger, D., Running, S., Anthoni, P., Bernhofer, C., Davis, S.K., Evans, R., Fuentes, J., Goldstein, A., Katul, G., Law, J.B., Lee, X., Malhi, Y., Meyers, T., Munger, W., Oechel, W., Paw, K.T., Pilegaard, K., Schmid, H.P., Valentini, R., Verma, S., Vesala, T., Wilson, K. and Wofsy, S. (2001) FLUXNET: a new tool to study the temporal and spatial

variability of ecosystem-scale carbon dioxide, water vapor, and energy flux densities. *Bulletin of the American Meteorological Society*, 82(11), 2415–2434.

Betts, A.K., Viterbo, P., Beljaars, A.C.M., Pan, H.-L., Hong, S.-Y., Goulden, M. and Wofsy, S. (1998) Evaluation of land-surface interaction in ECMWF and NCEP/NCAR reanalysis models over grassland (FIFE) and boreal forest (BOREAS). *Journal of Geophysical Research*, 103(D18), 23079–23085.

Bhat, G.S. and Fernando, H.J.S. (2016) Remotely driven anomalous sea–air heat flux over the north Indian Ocean during the summer monsoon season. *Oceanography*, 29, 232–241.

Bhat, G.S. and Narasimha, R. (2007) Indian summer monsoon experiments. *Current Science*, 93, 153–164.

Bhattacharya, B.K., Dutt, C.B.S. and Parihar, J.S. (2009) INSAT uplinked agromet station – a scientific tool with a network of automated micrometeorological measurements for soil canopy-atmosphere feedback studies. In: Panigrahy, S., Ray, S.S. and Parihar, J.S. (Eds.) *ISPRS Archives XXXVIII-8/W3 Workshop Proceedings: Impact of Climate Change on Agriculture, 17–18 December 2009, Ahmedabad, India*. Hanover, Germany: ISPRS, pp. 72–77. Available at: https://www.isprs.org/proceedings/XXXVIII/8-W3/ [Accessed 27th November 2019].

Bhattacharya, B.K., Singh, N., Bera, N, Nanda, MK, Bairagi, GD, Raja, P, Bal, SK, Muruga, V, Kandpal, BK, Patel, B.H. and Jain, A. (2013) *Canopy-scale dynamics of radiation and energy balance over short vegetative systems*. Available at: http://10.61.240.13:8080/jspui/handle/1/8404. Sci. Rep: SAC/EPSA/ABHG/IGBP/EME-VS/SR/02/2013.

Bollasina, M.A. and Ming, Y. (2013) The role of land-surface processes in modulating the Indian monsoon annual cycle. *Climate Dynamics*, 41, 2497–2509. https://doi.org/10.1007/s00382-012-1634-3.

CTCZ. (2008) *Continental tropical convergence zone (CTCZ) programme science plan*. Available at: http://www.incois.gov.in/documents/science_plan.pdf [Accessed 17th December 2018].

Fall, S., Watts, A., Nielsen-Gammon, J., Jones, E., Niyogi, D., Christy, J.R. and Pielke Sr, R.A. (2011) Analysis of the impacts of station exposure on the U.S. Historical Climatology Network temperatures and temperature trends. *Journal of Geophysical Research*, 116, D14120. https://doi.org/10.1029/2010JD015146.

Fratini, G. and Mauder, M. (2014) Towards a consistent eddy-covariance processing: an intercomparison of EddyPro and TK3. *Atmospheric Measurement Techniques*, 7, 2273–2281. https://doi.org/10.5194/amt-7-2273-2014.

Garratt, J.R. (1992) *The Atmospheric Boundary Layer*. *Cambridge Atmospheric and Space Sciences Series*. Cambridge, UK: Cambridge University Press.

Horst, T.W. and Weil, J.C. (1994) How far is far enough?: the fetch requirements for micrometeorological measurement of surface fluxes. *Journal of the Atmospheric and Oceanic Technology*, 11, 1018–1025.

Kljun, N., Calanca, P., Rotach, M.W. and Schmid, H.P. (2004) A simple parameterisation for flux footprint predictions. *Boundary-Layer Meteorology*, 112, 503–523.

Knupp, K.R. and Cotton, W.R. (1985) Convective cloud downdraft structure: an interpretive survey. *Reviews of Geophysics*, 23, 183–215.

Koster, R.D., Dirmeyer, P.A., Guo, Z., Bonan, G., Chan, E., Cox, P., Gordon, C.T., Kanae, S., Kowalczyk, E., Lawrence, D., Liu, P., Lu, C.-H., Malyshev, S., McAvaney, B., Mitchell, K., Mocko, D., Oki, T., Oleson, K., Pitman, A., Sud, Y.C., Taylor, C.M., Verseghy, D., Vasik, R., Xue, Y. and Yamada, T. (2004) Regions of strong coupling between soil moisture and precipitation. *Science*, 305, 1138–1140.

Lemone, M.A., Chen, F., Alfieri, J.G., Cuenca, R.H., Hagimoto, Y., Blanken, P., Niyogi, D., Kang, S., Davis, K. and Grossman, R.L. (2007) NCAR/CU surface, soil, and vegetation observations during the International H_2O Project 2002 field campaign. *Bulletin of the American Meteorological Society*, 88, 65–82. https://doi.org/10.1175/BAMS-88-I-65.

LI-COR Biosciences. (2016) *EddyPro® Software Instruction Manual*, 12th edition. Available at: www.licor.com/EddyPro [Accessed 21st November 2019].

LI-COR Biosciences. (2017) *Eddy Covariance Processing Software* (Version 6.2.1) [Software]. Available at: www.licor.com/EddyPro [Accessed 21st November 2019].

Niyogi, D. (2019) Land surface processes. In: Randall, D.A., Srinivasan, J., Nanjundaiah, R.S. and Mukhopadhyay, P. (Eds.) *Current Trends in the Representation of Physical Processes in Weather and Climate Models*. Singapore: Springer, pp. 349–370.

Padmanabhamurty, B. and Saxena, N. (2001) Variation of residual energy fluxes in relation to plant height and biomass in groundnut. *Journal of Agrometeorology*, 3, 107–118.

Rajeevan, M., Unnikrishnan, C.K. and Preethi, B. (2012) Evaluation of the ENSEMBLES multi-model seasonal forecasts of Indian summer monsoon variability. *Climate Dynamics*, 38, 2257–2274. https://doi.org/10.1007/s00382-011-1061-x.

Rajendran, K., Nanjundiah, R. and Srinivasan, J. (2002) Comparison of seasonal and intra-seasonal variation of tropical climate in NCAR CCM2 GCM with two different cumulus schemes. *Meteorology and Atmospheric Physics*, 79, 57–86.

Rajeshwari, A. and Mani, N.D. (2014) Estimation of land surface temperature of Dindigul district using Landsat 8 data. *International Journal of Research in Engineering and Technology*, 3, 122–126. https://doi.org/10.15623/ijret.2014.0305025.

Ren, H., Du, C., Liu, R., Qin, Q., Yan, G., Li, Z.L. and Meng, J. (2015) Atmospheric water vapor retrieval from Landsat 8 thermal infrared images. *Journal of Geophysical Research: Atmospheres*, 120, 1723–1738.

Rodell, M., Velicogna, I. and Famiglietti, J.S. (2009) Satellite-based estimates of groundwater depletion in India. *Nature*, 460, 999–1002. https://doi.org/10.1038/nature08238.

Saeed, F., Hagemann, S. and Jacob, D. (2009) Impact of irrigation on the South Asian summer monsoon. *Geophysical Research Letters*, 36, L20711. https://doi.org/10.1029/2009GL040625.

Sastry, P.S.N., Rao, P.S., Sheikh, A.M. and Pandey, V. (Eds.). (2001) Special issue on land surface processes experiment over Sabarmati River basin. *Journal of Agrometeorology*, 3, 1–26.

Shweta, Bhattacharya, B.K. and Krishna, A.P. (2018) A baseline regional evapotranspiration (ET) and change hotspots over Indian sub-tropics using satellite remote sensing data. *Agricultural Water Management*, 208, 284–298.

Sikka, D.R. and Narasimha, R. (1995) Genesis of the monsoon trough boundary layer experiment (MONTBLEX). *Proceedings of the Indian Academy of Sciences*, 104, 157–187.

Singh, N., Patel, N.R., Bhattacharya, B.K., Soni, P., Parida, B.R. and Parihar, J.S. (2014) Analyzing the dynamics and inter-linkages of carbon and water fluxes in subtropical pine (*Pinus roxburghii*) ecosystem. *Agricultural and Forest Meteorology*, 197, 206–218.

Sinha, S. and Pillai, J.S. (2001) Evaluation of moisture flux and relative humidity in the surface layer from sonic anemometer data. *Journal of Agrometeorology*, 3, 143–148.

Sundareshwar, V., Murtugudde, R., Srinivasan, G., Singh, S., Ramesh, K.J., Ramesh, R., Verma, S.B., Agarwal, D., Baldocchi, D., Baru, C.K., Baruah, K.K., Chowdhury, G.R., Dadhwal, V.K., Dutt, C.B.S., Fuentes, J., Gupta, P.K., Hargrove, W.W., Howard, M., Jha, C.S., Lal, S., Michener, M.K., Mitra, A.P., Morris, J.T., Myneni, R.R., Naja, M., Nemani, R., Purvaja, R., Raha, S., Santhana, S.K., Sharma, V.M., Subramaniam, A., Sukumar, R., Twilley, R.R. and Zimmerman, P.R. (2007) Environmental monitoring network for India. *Science*, 316, 204–205.

Taylor, C.M., Gounou, A., Guichard, F., Harris, P.P., Ellis, R.J., Couvreux, F. and De Kauwe, M. (2011) Frequency of Sahelian storm initiation enhanced over mesoscale soil-moisture patterns. *Nature Geoscience*, 4, 430–433. https://doi.org/10.1038/ngeo1173.

Turner, A.G., Bhat, G.S., Martin, G.M., Parker, D.J., Taylor, C.M., Mitra, A.K., Tripathi, S.N., Milton, S., Rajagopal, E.N., Evans, J.G., Morrison, R., Pattnaik, S., Sekhar, M., Bhattacharya, B.K., Madan, R., Govindankutty, M., Fletcher, J.K., Willetts, P.D., Menon, A., Marsham, J.H. and and the INCOMPASS team. (2019) Interaction of convective organization with monsoon precipitation, atmosphere, surface and sea: the 2016 INCOMPASS field campaign in India. *Quarterly Journal of the Royal Meteorological Society*, 2019, 1–25. https://doi.org/10.1002/qj.3633.

Wan, Z. (2014) New refinements and validation of the collection-6 MODIS land-surface temperature/emissivity products. *Remote Sensing of Environment*, 140, 36–45.

Webster, P.J., Bradley, E.F., Fairall, C.E., Godfrey, J.S., Hacker, P., Lucas, R., Serra, Y., Houze, R.A., Jr., Humman, J.M., Lawrence, T.D.M., Russel, C.A., Ryan, M.N., Sahami, K. and Zuidema, P. (2002) The joint air–sea interaction experiment (JASMINE): exploring intraseasonal variability in the South Asian monsoon. *Bulletin of the American Meteorological Society*, 83, 1603–1630.

Williams, M., Richardson, A.D., Reichstein, M., Stoy, P.C., Peylin, P., Verbeeck, H., Carvalhais, N., Jung, M., Hollinger, D.Y., Kattge, J., Leuning, R., Luo, Y., Tomelleri, E., Trudinger, C.M. and Wang, Y.-P. (2009) Improving land surface models with FLUXNET data. *Biogeosciences*, 6, 1341–1359. https://doi.org/10.5194/bg-6-1341-2009.

Yasunari, T. (2006) Land–atmosphere interaction. In: Wang, B. (Ed.) *The Asian Monsoon*. Berlin, Germany: Springer-Verlag, pp. 459–477.

SUPPORTING INFORMATION

Additional supporting information may be found online in the Supporting Information section at the end of this article.

How to cite this article: Bhat GS, Morrison R, Taylor CM, Bhattacharya BK, Paleri S, Desai D, Evans JG, Pattnaik S, Sekhar M, Nigam R, Sattar A, Angadi SS, Kacha D, Patidar A, Tripathi SN, Krishnan KVM, Sisodiya A. Spatial and temporal variability in energy and water vapour fluxes observed at seven sites on the Indian subcontinent during 2017. *Q J R Meteorol Soc*. 2019;1–14. https://doi.org/10.1002/qj.3688